JCI The Journal of Clinical Investigation

Homeostatically proliferating CD4+ T cells are involved in the pathogenesis of an Omenn syndrome murine model

Khie Khiong, … , Philippa Marrack, Toshio Hirano

J Clin Invest. 2007;117(5):1270-1281. https://doi.org/10.1172/JCI30513.

Research Article

Patients with Omenn syndrome (OS) have hypomorphic *RAG* mutations and develop varying manifestations of severe combined immunodeficiency. It is not known which symptoms are caused directly by the *RAG* mutations and which depend on other polymorphic genes. Our current understanding of OS is limited by the lack of an animal model. In the present study, we identified a C57BL/10 mouse with a spontaneous mutation in, and reduced activity of, RAG1. Mice bred from this animal contained high numbers of memory-phenotype T cells and experienced hepatosplenomegaly and eosinophilia, had oligoclonal T cells, and demonstrated elevated levels of IgE, major symptoms of OS. Depletion of $CD4^+$ T cells in the mice caused a reduction in their IgE levels. Hence these “memory mutant” mice are a model for human OS; many symptoms of their disease were direct results of the *Rag* hypomorphism and some were caused by malfunctions of their $CD4^+$ T cells.

 Related Commentary, page 1213

Homeostatically proliferating CD4+ T cells are involved in the pathogenesis of an Omenn syndrome murine model

Khie Khiong,[1] Masaaki Murakami,[1,2] Chika Kitabayashi,[1] Naoko Ueda,[1] Shin-ichiro Sawa,[1] Akemi Sakamoto,[2] Brian L. Kotzin,[3] Stephen J. Rozzo,[3] Katsuhiko Ishihara,[1] Marileila Verella-Garcia,[4] John Kappler,[2] Philippa Marrack,[2] and Toshio Hirano[1,5]

[1]Department of Developmental Immunology, Graduate School of Medicine and Graduate School of Frontier Biosciences, Osaka University, Osaka, Japan. [2]Integrated Department of Immunology, University of Colorado Health Sciences Center, Howard Hughes Medical Institute, and National Jewish Medical and Research Center, Denver, Colorado, USA. [3]Division of Clinical Immunology, University of Colorado Health Sciences Center, Denver, Colorado, USA. [4]Lung Cancer Program, Department of Medicine, University of Colorado Cancer Center, Denver, Colorado, USA. [5]Laboratory of Cytokine Signaling, RIKEN Research Center for Allergy and Immunology, Yokohama, Japan.

Patients with Omenn syndrome (OS) have hypomorphic *RAG* mutations and develop varying manifestations of severe combined immunodeficiency. It is not known which symptoms are caused directly by the *RAG* mutations and which depend on other polymorphic genes. Our current understanding of OS is limited by the lack of an animal model. In the present study, we identified a C57BL/10 mouse with a spontaneous mutation in, and reduced activity of, RAG1. Mice bred from this animal contained high numbers of memory-phenotype T cells and experienced hepatosplenomegaly and eosinophilia, had oligoclonal T cells, and demonstrated elevated levels of IgE, major symptoms of OS. Depletion of CD4+ T cells in the mice caused a reduction in their IgE levels. Hence these "memory mutant" mice are a model for human OS; many symptoms of their disease were direct results of the *Rag* hypomorphism and some were caused by malfunctions of their CD4+ T cells.

Introduction

During lymphocyte development, B cell receptor (BCR) and TCR genes are assembled in developing lymphocyte precursors by a process known as V(D)J recombination, which is caused by activation of the Rag1 and Rag2 proteins (1–6). Disruption of Rag1 or Rag2 blocks this recombination and leads to the complete absence of mature B and T cells (7, 8). Mutations in humans that eliminate the recombination activity of RAG1 or RAG2 lead to SCID (9). However, SCID has several forms in humans, which are caused by defects in different genes. For example, the autosomal-recessive genetic disorder Omenn syndrome (OS) is characterized by low levels of mature B cells and normal to increased numbers of activated T cells and is associated with erythroderma, eosinophilia, hepatosplenomegaly, lymphadenopathy, and elevated serum IgE levels (10, 11). Patients with this syndrome frequently suffer from alopecia, chronic diarrhea, failure to thrive, and recurrent infections; these symptoms usually lead to death unless the OS is treated successfully by bone marrow or cord blood stem cell transplantation (12).

Most OS patients have mutations in one of the *RAG* genes. These mutations lead to the partial loss of recombination activity in precursor B and T cells and lowered production of these cells, the latter of which may be the underlying defect causing the disease. Thus, the distinction between patients with OS and those with SCID but not OS may depend on the severity of the *RAG* mutation (13–15), with very severe mutations causing complete SCID and partial defects in RAG activity leading to OS. However, the symptoms of OS vary somewhat from patient to patient, and it is unknown which consequences of the *RAG* mutation are direct and which are indirect. Understanding of the disease has so far been limited by the absence of a suitable animal model.

Here we report the characteristics of the memory mutant (MM) strain of mice, which were found to have an unusually high percentage of memory-phenotype T cells. The phenotype of the MM mouse was inherited in an autosomal-recessive manner, and MM hematopoietic cells transmitted the phenotype. The MM phenotype was caused by a point mutation in *Rag1*, which decreased its V(D)J recombination activity. T and B cell development in MM mice was partially blocked at the step where Rag-mediated rearrangement was required. The MM mice had many symptoms in common with OS patients, including skin redness, hepatosplenomegaly, eosinophilia, oligoclonal Vβ usage in T cells, and elevated serum IgE levels. This last characteristic, which is the critical symptom for the differential diagnosis of OS versus SCID patients, was alleviated in MM mice by depletion of their CD4+ T cells. In addition, CD4+ T cells in MM mice expressed unusually high levels of cytokines and underwent homeostatic proliferation, even without treatment to induce further lymphopenia. However, while most OS patients develop symptoms of disease early in life, the MM mice developed symptoms relatively late in life. These symptoms might be accelerated in humans with OS by interactions between the *RAG* mutations and environmental factors or by other genetic polymorphisms. Thus, we conclude that the MM mouse is a murine model of OS and that dysregulated homeostatic proliferating CD4+ T cells are involved in the pathogenesis of this OS murine model.

Nonstandard abbreviations used: BCR, B cell receptor; DN, double negative; FACS, fluorescence-activated cell sorter; IL-2R, IL-2 receptor; OS, Omenn syndrome; MM, memory mutant; MTT, 3-(4,5-dimethyl-2-thiazolyl)-2,5-diphenyl-2H-tetrazolium bromide; TD, thymus dependent; TI, thymus independent.

Conflict of interest: The authors have declared that no conflict of interest exists.

Citation for this article: *J. Clin. Invest.* **117**:1270–1281 (2007). doi:10.1172/JCI30513.

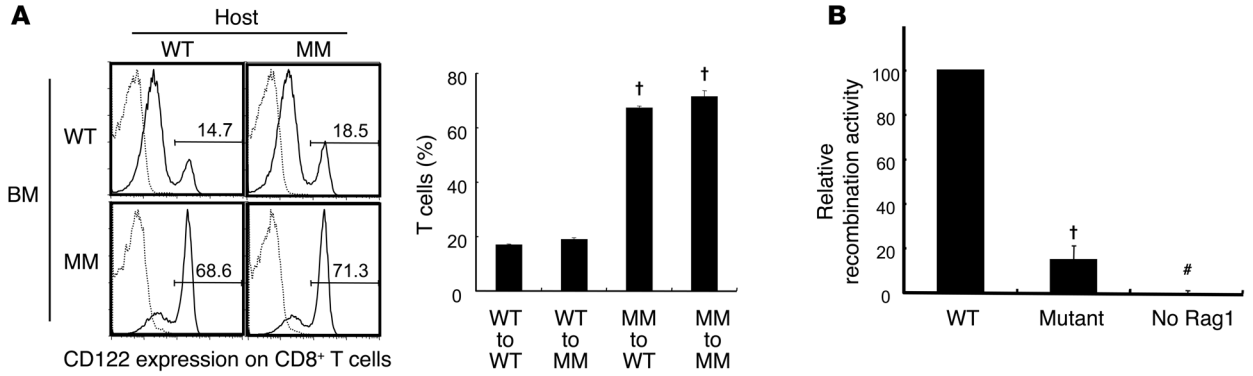

Figure 1
Discovery of a spontaneous mutant, the MM mouse, which carries a hypomorphic *Rag* mutation. (**A**) Bone marrow transplantation was performed using bone marrow from wild-type or MM mice transplanted into lethally irradiated wild-type or MM hosts. The percentage of memory-phenotype CD8+ T cells in PBLs was determined 3–4 months after transplantation. Numbers denote percentage of cells within the ranges indicated by brackets. Results are mean and SD of 4 mice. The percentage of CD8+ T cells that were $CD122^{high}$ increased in the wild-type and MM mice ($P < 0.001$) that received transplants of MM bone marrow. (**B**) Recombination activity of Rag1 from wild-type and MM mice. Results are mean and SD of 6 experiments. The recombination activity of Rag1 decreased in MM mice ($P < 0.001$) and mice with Rag2 alone (i.e., no Rag1; $P = 0.003$) compared with wild-type mice. $^{\#}P < 0.01$, $^{\dagger}P < 0.001$ versus wild type.

Results

Discovery of a spontaneous mutant mouse carrying a hypomorphic Rag mutation. During a routine analysis of the mechanisms underlying memory-phenotype T cell development in vivo, we investigated the percentage of memory-phenotype CD8+ T cells in over 300 normal mice of various ages, obtained from The Jackson Laboratory. We found a female C57BL/10 mouse with an abnormally high percentage of memory-phenotype CD8+ T cells (Supplemental Figure 1; supplemental material available online with this article; doi:10.1172/JCI30513DS1). The mutant mouse did not have any detectable infections, was being maintained under specific pathogen–free conditions at the National Jewish Medical and Research Center, appeared healthy, and was indistinguishable from her normal littermates by visual inspection. The F1 offspring from the mutant mouse crossed with a wild-type C57BL/10 male mouse had no unusual phenotypes. However, about 22%–23% of the F2 offspring from the F1 intercrosses had high percentages of memory-phenotype CD8+ T cells. Therefore, we concluded that the phenotype of this mouse, which we termed the MM mouse, was inherited in an autosomal-recessive manner.

To determine whether the mutant phenotype of MM mice was dependent on a defect in the precursor cells of the bone marrow or on nonhematopoietic cells, we performed bone marrow transplantations of all combinations of MM and wild-type C57BL/10 mice. In the 2 groups of chimeric mice containing MM hematopoietic cells, the number of memory-phenotype CD8+ T cells increased regardless of whether the nonhematopoietic cells had the mutation (Figure 1A). These results indicated that the phenotype of the CD8+ T cells was dependent on the donor hematopoietic cells and not on the nonhematopoietic cells in their environment.

In order to identify the mutation responsible for the phenotype of the MM mice, we first performed a cytogenetic Giemsa-trypsin-Leishman (GTL) banding analysis using activated T cells from the MM mice. However, we observed no structural abnormalities or variants (Supplemental Figure 2). Next, we outcrossed the MM mouse with the NZB strain, and the F1 progeny were then intercrossed to produce F2 offspring with or without the CD8+ T cell phenotype. PCR was performed using genomic DNA from the F2 mice with simple sequence length polymorphism (SSLP) markers. We found that the locus carrying the mutation mapped to chromosome 2. We then narrowed down the locus using other SSLP markers for chromosome 2 and found the mutation to be between D2Mit333 and D2Mit473 (data not shown). This locus contained 42 candidate genes, as shown in Supplemental Table 1.

We sequenced the full-length cDNAs from the 42 candidates and found 1 nucleotide substitution in the *Rag1* gene of the MM mouse. This point mutation changed an arginine to glutamine at residue 972 in the core domain of the Rag1 protein (Supplemental Figure 3).

We hypothesized that this point mutation was responsible for the phenotype of the MM mice, because an amino acid substitution in the core domain of a Rag protein usually reduces its rearranging activity. To test this hypothesis, we used an in vitro recombination assay (6) and found that the mutant Rag from the MM mice had weak recombination activity (about 12%) compared with that from wild-type mice (Figure 1B). These results indicated that the point mutation in the *Rag1* gene partially decreased the V(D)J recombination activity in the MM mice; moreover, they strongly suggested that the MM mouse could be a model for OS, because OS in humans is caused by reduced recombination activity of Rag molecules (13–15). The *Rag* mutation might have also affected Rag activity in the mice by reducing the stability of the protein. To determine whether the levels of Rag1 protein were reduced in MM versus wild-type mice, we prepared lysates from $CD4^-CD8^-$ double-negative (DN) thymus cells and $B220^+$ bone marrow cells from MM and wild-type mice. The amount of Rag1 protein per unit of cells was almost the same regardless of whether the cells came from MM or wild-type mice (Supplemental Figure 4). Therefore, we concluded that the *Rag1* mutation in MM mice did not reduce the stability of the protein.

MM mice provide a murine model of OS. Rag-mediated rearrangement is critical for the development of T and B cells (7, 8). Therefore, it was important to determine whether the decreased Rag activity in MM mice inhibited T and B cell development. Staining

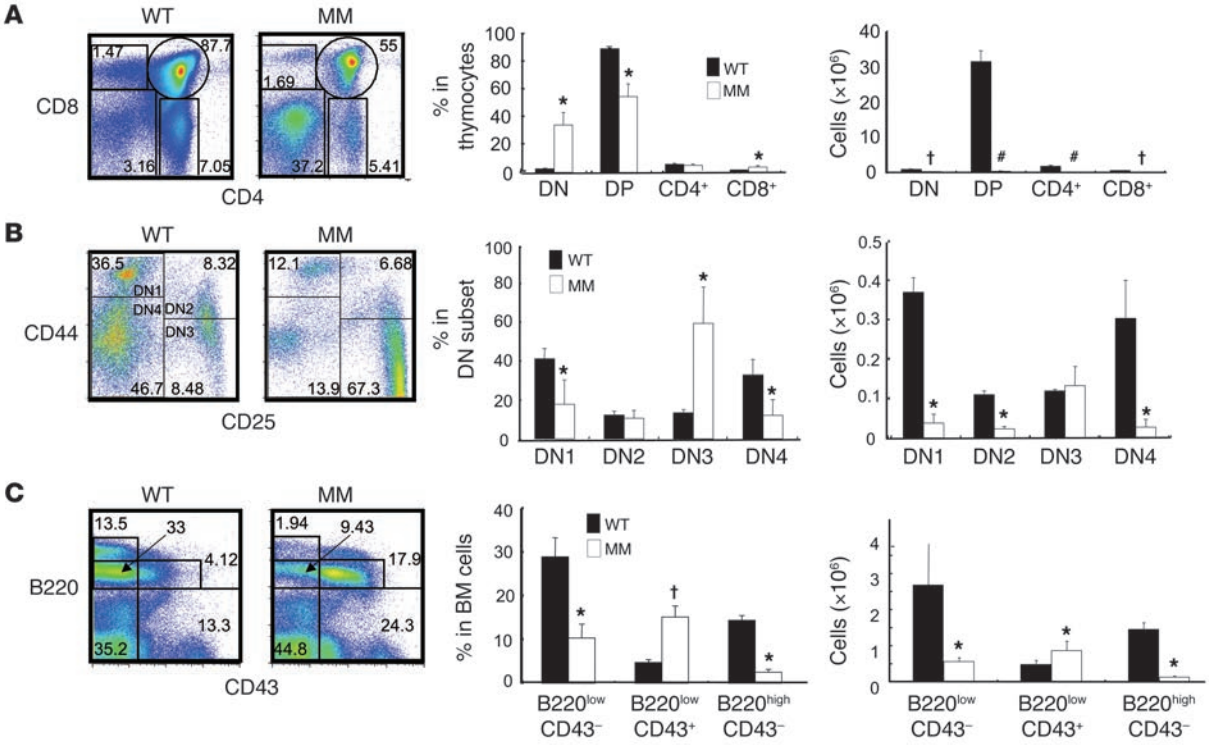

Figure 2
T and B cell development in MM mice is inhibited at receptor gene rearrangement stages. (**A**) The percentage of DN cells was higher ($P = 0.03$), while the actual number of DN ($P < 0.001$), double-positive (DP; $P = 0.003$), CD4+ ($P = 0.008$), and CD8+ ($P < 0.001$) thymocytes was lower, in MM compared with wild-type mice. Numbers denote percentage of cells within the indicated gates. (**B**) The percentage of DN3 cells was higher in MM mice than in wild-type mice ($P = 0.01$), while the actual cell numbers were comparable. (**C**) The percentage ($P < 0.001$) and number ($P = 0.02$) of B220^{low}CD43+ cells was higher in MM than in wild-type mice. *$P < 0.05$, #$P < 0.01$, †$P < 0.001$ versus wild type.

of thymocytes showed that the percentage of CD4+CD8+ double-positive cells was markedly decreased, and that of CD4−CD8− DN cells was significantly increased, in the MM versus wild-type mice (Figure 2A). Thus T cell development in the MM mice was partially blocked at the DN stage. Examination of the frequency of different populations of DN cells in the thymi of these mice revealed that the blockade occurred at the DN3 stage, the stage at which Rag-mediated rearrangement of the TCR-β gene is required (Figure 2B). B cell development was also partially blocked in the MM mice, again at the stage at which Rag is first needed to act, in the CD43+B220^{med} fraction of pro-B cells (Figure 2C); further development requires Rag-mediated rearrangement of the μ heavy-chain gene.

It has previously been reported that OS patients have a reduced number of B cells and normal to elevated numbers of activated T cells in the periphery (10, 11). Consistent with these reports, the percentage of IL-2 receptor β– and CD44-high (IL-2Rβ^{high}CD44^{high}) memory-phenotype CD4+ and CD8+ T cells and IL-2Rα+CD69+ activated-phenotype CD4+ T cells was higher than normal in the spleens of MM mice (Figure 3, A and B). Conversely, the actual number of both CD4+ and CD8+ T cells was lower in MM than in wild-type mice (Figure 3B). In addition, both the percentage and the actual number of IgM+ B cells were lower in the spleens and bone marrow of the MM mice than in those of wild-type mice (Figure 3C). However, the percentage of cells that were B220+IgM− (pre-B cells) in B220+ cells was high in the bone marrow of the MM mice (about 69% in controls and about 92% in MM mice; Figure 3C). The spleens of MM mice had a greater percentage of pre-B cells but a smaller percentage of immature B cells than did the spleens of wild-type mice. To investigate whether the IgM+ B cells detected in the spleens of MM mice were oligoclonal, we performed spectratyping of IgM using spleen cells. The results showed that some V_hJ558 and V_hQ52 family genes had restricted spectratypes, suggesting that they were expressed in an oligoclonal manner (Figure 4A).

Consistent with the reduction in total T and B cell numbers, the actual number of cells was significantly reduced in the spleens, lymph nodes, and thymi of the MM mice, but not in the bone marrow (Figure 4B). The architecture of these organs in MM mice was also abnormal. The white pulp in the spleen and lymphoid follicles of lymph nodes was diffuse and contained fewer lymphocytes in MM than in wild-type mice (Supplemental Figure 5). Examination of thymi showed that the thymus medullae of MM mice were small and, consequently, that most of the thymus in these mice was composed of cortex (Supplemental Figure 5).

In order to determine how the properties of individual lymphocytes were affected in the MM mice, we evaluated the proliferation of T and B cells from MM and wild-type mice after stimulation with LPS for B cells or with anti-CD3 and anti-CD28 for T cells. B cells from MM mice proliferated more vigorously than did wild-type B cells in the absence of any added stimulus and in response to low levels of LPS (Figure 4C). Only in the pres-

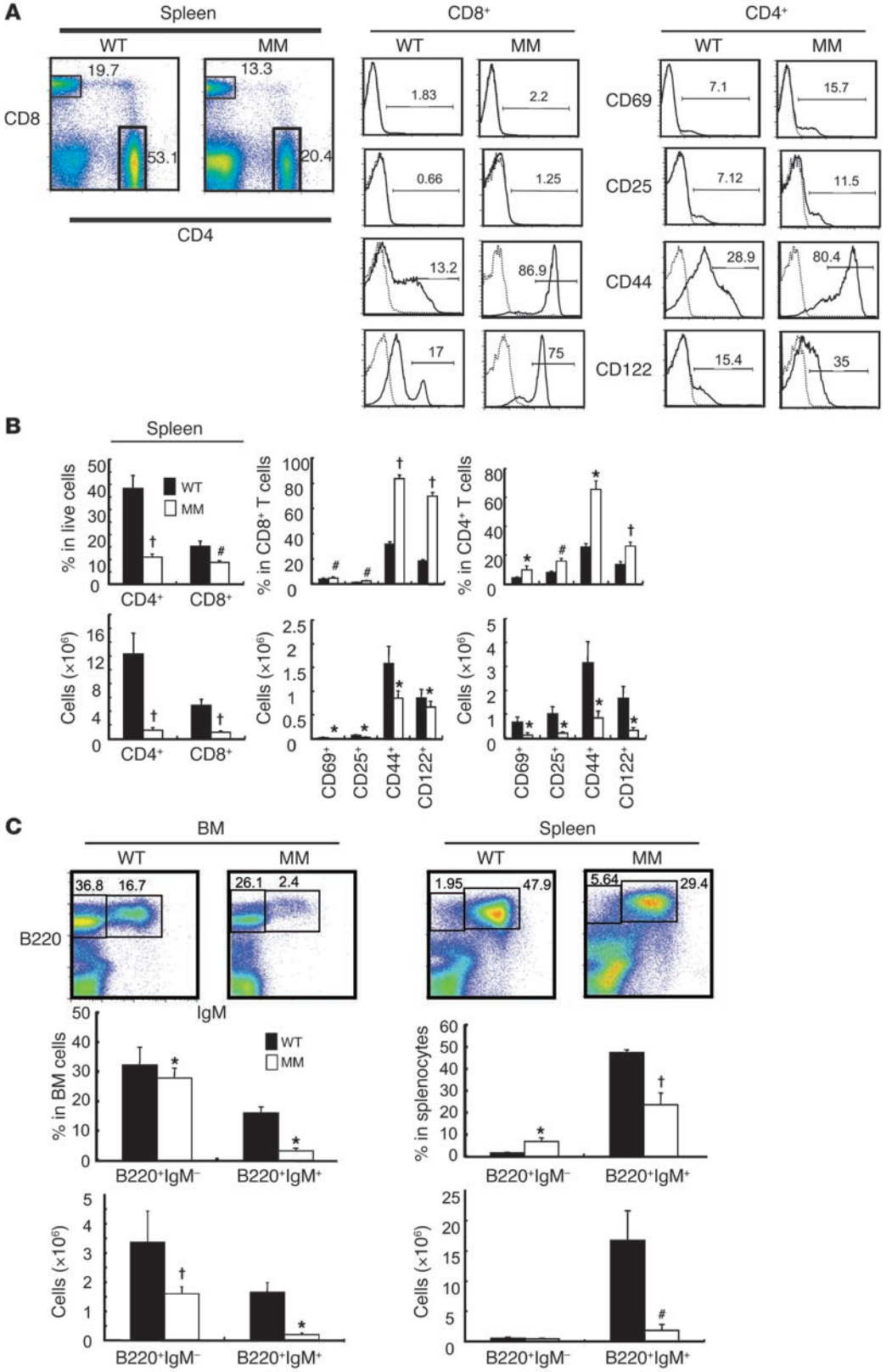

Figure 3
T and B cell development in MM mice is inhibited at receptor gene rearrangement stages. (**A**) The memory/activated phenotype of CD4+ and CD8+ T cells in the spleen was analyzed by FACS. Numbers denote percentage of cells within the indicated gates or bracketed ranges. (**B**) The percentage and number of CD4+ ($P < 0.001$ and $P < 0.001$, respectively) and CD8+ ($P = 0.001$ and $P < 0.001$, respectively) T cells in the spleen was lower in MM than in wild-type mice. The percentages of CD8+CD69+ ($P = 0.006$), CD8+CD25+ ($P = 0.001$), CD8+CD44+ ($P < 0.001$), CD8+CD122+ ($P < 0.001$) and CD4+CD69+ ($P = 0.02$), CD4+CD25+ ($P = 0.001$), CD4+CD44+ ($P = 0.02$), and CD8+CD122+ ($P < 0.001$) cells were higher in MM than in wild-type mice. Data were calculated using the FACS profiles in **A**. (**C**) The percentage and number of bone marrow B220+IgM− ($P = 0.03$ and $P < 0.001$, respectively) and B220+IgM+ ($P = 0.01$ and $P = 0.02$, respectively) cells as well as splenic B220+IgM+ cells ($P < 0.001$ and $P = 0.002$, respectively) were lower in MM mice than in wild-type mice. *$P < 0.05$, #$P < 0.01$, †$P < 0.001$ versus wild type.

ence of high concentrations of LPS did the MM and wild-type B cells respond equivalently (Figure 4C). The proliferation of MM T cells was significantly reduced compared with that of T cells from wild-type controls (Figure 4, C and D). Similar abnormalities have been reported for T cells from OS patients; it has also been demonstrated that the degrees of reduction in the T cell

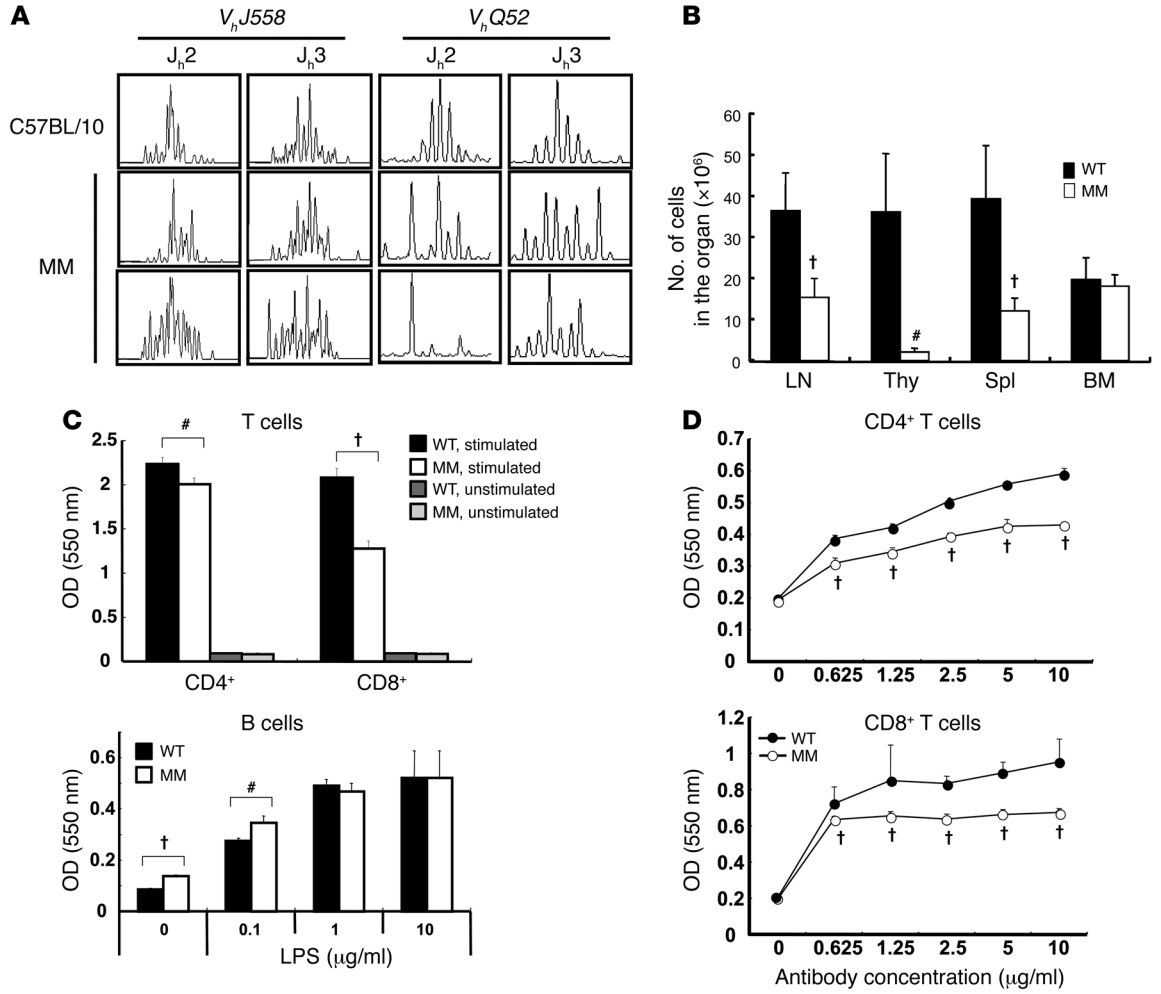

Figure 4

T and B cell development in MM mice is inhibited at receptor gene rearrangement stages. (**A**) Spectratypes of V_hJ558 and V_hQ52 family genes were performed using splenocytes from MM mice and C57BL/10 controls. Representative data are shown. (**B**) The number of cells in the MM mouse lymph nodes (inguinal, axillaries, cervical, and mesenteric; $P < 0.001$), thymus (Thy; $P = 0.005$), and spleen (Spl; $P < 0.001$) than in those of wild-type mice. Results are mean and SD of 5–6 mice (6–9 weeks old). (**C** and **D**) $CD4^+$ and $CD8^+$ T cells were sorted from spleens and lymph nodes of MM and control mice and stimulated by 10 μg/ml (**C**, top) and indicated concentrations of anti-CD3 and anti-CD28 (**D**). MTT assay showed less T cell proliferation in MM than in wild-type cells (stimulated $CD4^+$, $P = 0.002$; stimulated $CD8^+$, $P < 0.001$; $CD4^+$ and $CD8^+$ at all concentrations, $P < 0.001$). (**C**, bottom) $B220^+CD19^+$ B cells were sorted from spleens of MM and control mice and stimulated by indicated concentrations of LPS. MTT assay showed more B cell proliferation in MM than in wild-type cells stimulated with 0 μg/ml LPS ($P < 0.001$) or 0.1 μg/ml LPS ($P = 0.001$). $^{\#}P < 0.01$, $^{\dagger}P < 0.001$ versus wild type.

responses from OS patients had variations from absent to normal compared with T cells from healthy volunteers (15–20).

Patients with OS have few B cells and low levels of serum Ig. To find out how effectively antibodies can be raised in MM mice, we immunized both MM and wild-type mice with thymus-dependent (TD) or thymus-independent (TI) antigen (2,4-dinitrophenyl–keyhole limpet hemocyanin [DNP-KLH] or 2,4,6-trinitrophenyl–LPS [TNP-LPS], respectively; see Methods). The 2 types of mice generated comparable levels of anti-DNP or anti-TNP antibodies at all time points analyzed (Supplemental Figures 6 and 7). We also assessed the percentages and numbers of splenic germinal center B cells in MM and wild-type mice in the presence and absence of antigen challenge by using their surface markers ($B220^+IgM^-IgD^-GL\text{-}7^+PNA^+$). Interestingly, in the resting state prior to antigen challenge, MM mice had 6 times more germinal center B cells than did wild-type controls (Supplemental Figure 8). However, the percentage and actual number of germinal center B cells barely increased in MM mice as a result of immunization with the TD antigen, while immunization with the TD antigen doubled the number of these cells in wild-type controls (Supplemental Figure 8). Thus MM mice were less B cell deficient than are patients with OS, and the B cells in these mice can respond appropriately to antigen and T cell help.

The major symptoms of OS are erythroderma, lymphadenopathy, hepatosplenomegaly, hypereosinophilia, hypogammaglobulinemia, oligoclonal T cells, an elevated serum IgE level, and immunodeficiency, although the symptoms vary somewhat from patient to patient. To understand this disease better, it is important to know which symptoms are the direct results of the *Rag* mutation. We found that at all time points analyzed, MM mice had higher

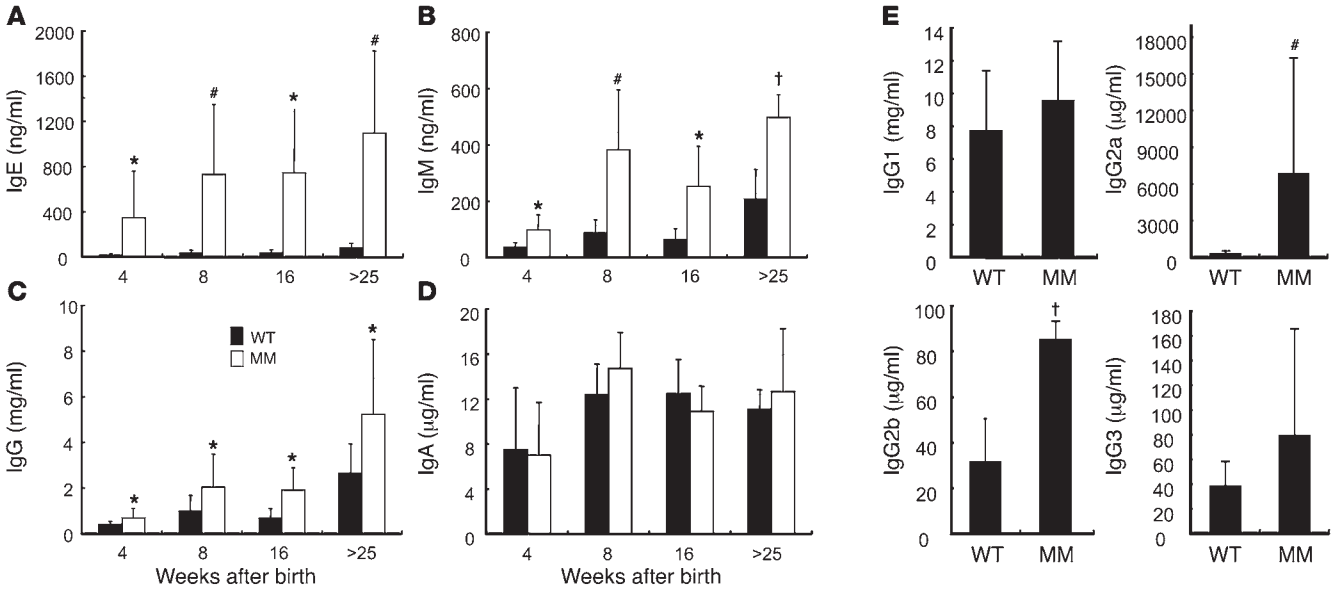

Figure 5

MM have high serum concentrations of IgE, IgM, IgG, and IgA. (**A**–**D**) Sera from wild-type and MM mice of different ages were collected and their IgE (**A**), IgM (**B**), IgG (**C**), and IgA (**D**) concentrations were analyzed. Results are mean and SD of 15 mice. At all ages tested, the serum concentration of IgE (4 wk, $P = 0.04$; 8 wk, $P = 0.002$; 16 wk, $P = 0.03$; >25 wk, $P = 0.002$), IgM (4 wk, $P = 0.01$; 8 wk, $P = 0.002$; 16 wk, $P = 0.01$; >25 wk, $P < 0.001$), and IgG (4 wk, $P = 0.02$; 8 wk, $P = 0.03$; 16 wk, $P = 0.02$; >25 wk, $P = 0.04$) was higher in MM than in wild-type mice. (**E**) Serum concentrations of IgG1, IgG2a, IgG2b, and IgG3 were also measured. Results are mean and SD of 30 mice. The serum concentrations of IgG2a ($P = 0.004$) and IgG2b ($P < 0.001$) were higher in MM than in wild-type mice. $^{*}P < 0.05$, $^{\#}P < 0.01$, $^{\dagger}P < 0.001$ versus wild type.

serum levels not only of IgE (by more than 1,000-fold), but also of IgG, IgM, IgG2a, and IgG2b, compared with controls (Figure 5, A–C and E). However, the serum IgA levels were comparable between wild-type and MM mice (Figure 5D).

MM mice had a significant elevation in the percentage of eosinophils ($CCR3^{high}Gr\text{-}1^{low}$) in PBLs (Figure 6A). The skin of infant MM mice was red compared with that of wild-type mice (Figure 6B), although we did not observe infiltration of the skin by activated T lymphocytes and eosinophils (Supplemental Figure 5), suggesting increased vessel permeability in MM mice. We also observed splenomegaly and hepatomegaly, but not lymphadenopathy, in aged MM mice (Figure 6, C–F). There was significantly perturbed TCRVβ and TCRVα usage in the MM mice, as assessed by anti-TCRVβ antibody or spectratyping analysis (Figure 6, G and H). The results of these analyses suggested that the T cells in MM mice were oligoclonal. Hematological analysis of the peripheral blood of MM mice showed a reduction in the number of white blood cells, especially lymphocytes, but not of other cell populations, including red blood cells and platelets, compared with controls (Supplemental Figure 9). Because all the symptoms described here are also seen in OS patients, we conclude that the MM mice provide a novel animal model for OS.

The environment in MM mice promotes homeostatic expansion of T cells, and MM T cells are involved in the production of high levels of IgE. There were very few T cells in MM mice (Figure 3B). In other models, lymphopenia of this magnitude has been associated with spontaneous proliferation on the part of the remaining T cells in the animals, a process termed homeostatic proliferation. The proliferating T cells also acquire activation markers and the ability to produce some cytokines (21). This proliferation is though to be caused by cytokines, such as IL-7 and interaction with MHC proteins and self peptides. To determine whether the environment in MM mice allows homeostatic proliferation and thus perhaps causes the activated phenotype of their T cells, $CD4^{+}$ and $CD8^{+}$ T cells from C57BL/6 mice were purified, labeled with CFSE, and transferred to 3-day-old neonatal and 8-week-old adult MM and wild-type mice. Three weeks later, T cells were isolated from the mice and analyzed for dilution of their CFSE label. Almost none of the T cells transferred to wild-type mice had divided regardless of their source. After transfer to MM mice, however, both MM and wild-type T cells divided (Figure 7, A and B). This was true for transfers to both neonatal and adult mice. These results suggest that the lymphopenic environment in MM mice promotes homeostatic expansion of T cells, which may cause their activated phenotype and production of cytokines by the cells.

The clinical and immunological features of OS have been related to an unbalanced expansion of the Th2 cell subset (12). In addition, we and others have previously shown that the homeostatic proliferation of $CD4^{+}$ T cells is critical for the development of a number of diseases, including autoimmunity (22, 23). We hypothesized that the homeostatically proliferating $CD4^{+}$ T cells express excess amounts of Th2 cytokines and play a role in the development of symptoms observed in MM mice. The $CD4^{+}$ T cells of MM mice produced large amounts of Th2 cytokines, including IL-4 and IL-6, compared with those of wild-type controls (Figure 7C). Together with the increased expression of activation markers on the $CD4^{+}$ T cells of MM mice (Figure 1), these results demonstrated that the homeostatic proliferating $CD4^{+}$ T cells in MM mice were activated and produced large amounts of Th2 cytokines. Moreover, we analyzed expression of activation markers and cytokines in adoptively transferred T cells derived from wild-type mice and found that even wild-type $CD4^{+}$ T cells transferred in

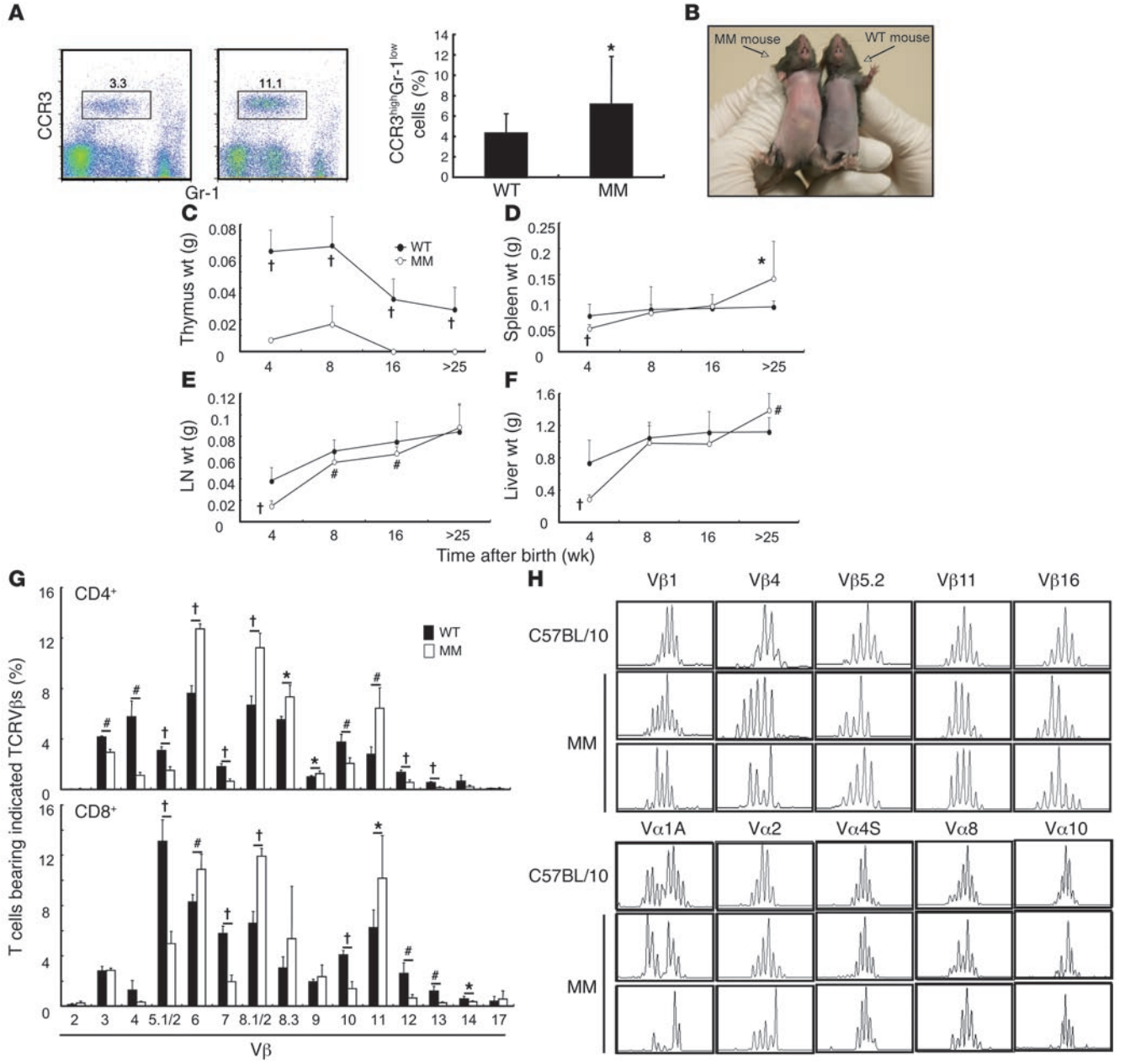

Figure 6

MM mice have symptoms similar to those of OS patients. (**A**) The percentage of eosinophils ($CCR3^{high}Gr\text{-}1^{low}$), as determined using PBLs of wild-type and MM mice, was greater in MM than in wild-type mice. Results are mean and SD of 12 mice. (**B**) To examine the skin of wild-type and MM mice, their abdominal hair was shaved. Panel shows the skin color of wild-type and MM mice, typical of more than 10 analyzed. (**C**–**F**) Weights of the thymus (**C**), spleen (**D**), lymph nodes (**E**), and liver (**F**) at the indicated time points were higher in MM than in wild-type mice. Results are mean and SD of more than 50 mice. (**G**) Vβ usage by $CD4^+$ and $CD8^+$ T cells in 8-week-old wild-type and MM mice was measured by FACS analysis. Results are mean and SD of 5 mice. The percentage of $V\beta3^+$, $V\beta4^+$, $V\beta5.1^+5.2^+$, $V\beta7^+$, $V\beta10^+$, $V\beta12^+$, and $V\beta13^+$ $CD4^+$ cells and of $V\beta5.1^+5.2^+$, $V\beta7^+$, $V\beta10^+$, $V\beta12^+$, $V\beta13^+$, and $V\beta14^+$ $CD8^+$ cells was lower, while the percentage of $V\beta6^+$, $V\beta8.1^+8.2^+$, $V\beta8.3^+$, $V\beta9^+$, and $V\beta11^+$ $CD4^+$ cells and of $V\beta6^+$, $V\beta8.1^+8.2^+$, and $V\beta11^+$ $CD8^+$ cells was higher, in MM compared with wild-type mice. (**H**) Spectratypes of Vα and Vβ family genes were performed using splenocytes from MM mice and C57BL/10 controls. Representative data are shown. $^*P < 0.05$, $^{\#}P < 0.01$, $^{\dagger}P < 0.001$ versus wild type.

MM mice expressed high level of activation markers CD44 and CD69 and Th2 cytokines IL-4 and IL-6 (Figure 7D), which indicates that a lymphopenic condition in MM mice activates normal $CD4^+$ T cells to express cytokines in vivo.

To prove the importance of homeostatic proliferating $CD4^+$ T cells in inducing symptoms in the MM mouse model of OS, we established double-mutant MM mice that lacked CD4 T cells. We investigated the serum IgE level in these double mutants,

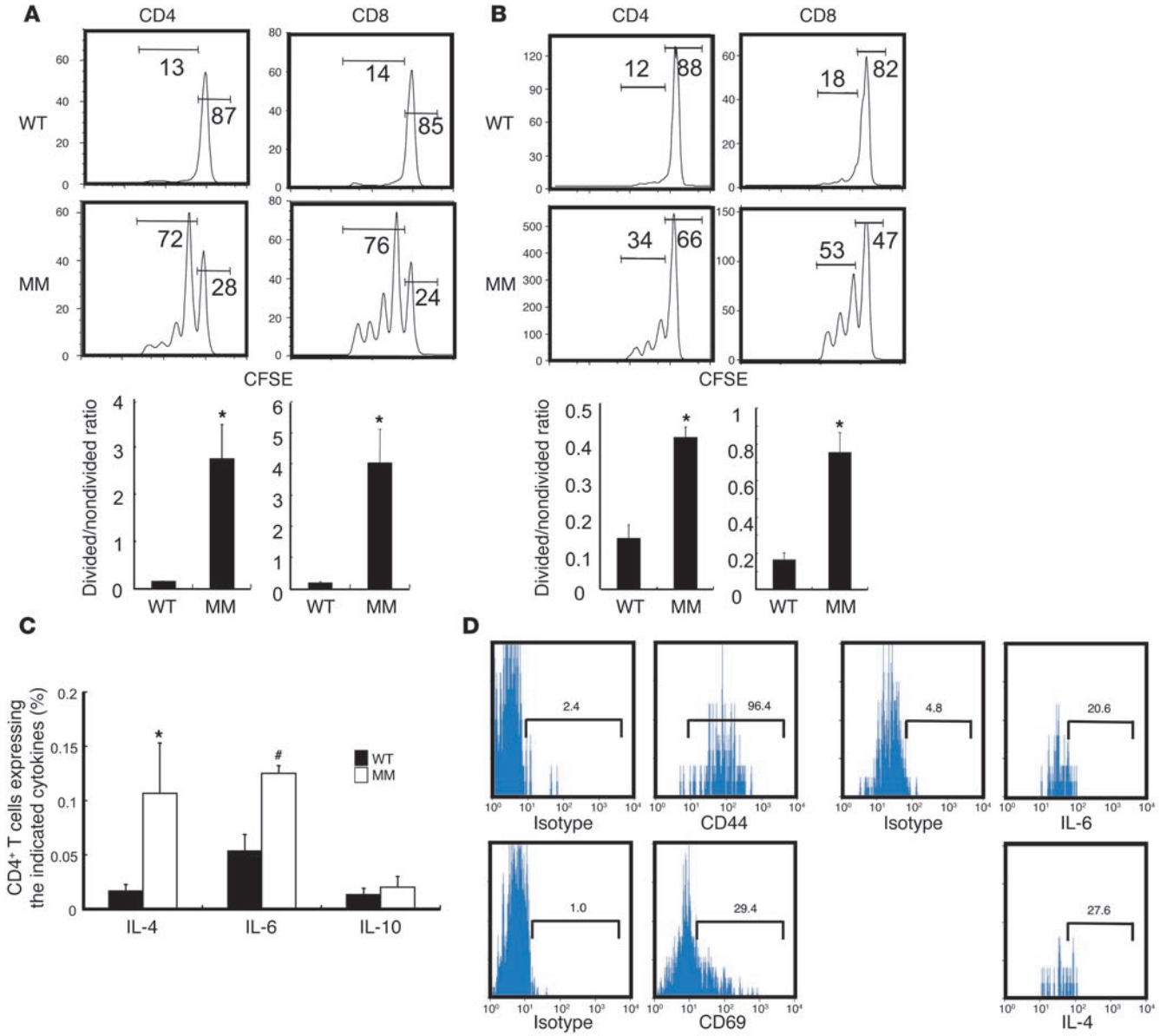

Figure 7

Homeostatically proliferating CD4+ T cells express high amounts of Th2 cytokines and are involved in the hyper-IgE status of MM mice. (**A** and **B**) CD4+ and CD8+ T cells of the naive phenotype ($CD44^{low}$) from normal C57BL/10 mice were sorted, labeled with CFSE, and transferred into nonirradiated wild-type and nonirradiated MM 3-day-old (**A**) and 8-week-old (**B**) mice. Homeostatic proliferation of CD4+ and CD8+ cells in the spleen and lymph nodes was investigated by FACS analysis and dilution of the CFSE label. Results are mean and SD of 6 mice. This ratio of divided to nondivided cells was higher in MM than in wild-type mice both at 3 days (CD4+, $P = 0.02$; CD8+, $P = 0.03$) and at 8 weeks (CD4+, $P = 0.01$; CD8+, $P = 0.02$). (**C**) Intracellular cytokine staining was performed using the CD4+ T cells of 8-week-old wild-type and MM mice and analyzed by FACS. Results are mean and SD of 10 mice. The percentage of cells positive for several cytokines was higher in MM than in wild-type mice (IL-6, $P = 0.009$; IL-4, $P = 0.03$). (**D**) CD4+ T cells of the naive phenotype ($CD44^{low}$) from normal C57BL/6 SJL ($CD45.1^{+}$) mice were sorted (99% purity), labeled with CFSE, and transferred into nonirradiated MM mice 8 weeks after birth. Eight days after transfer, CFSE-$CD45.1^{+}$ cells in the spleen and lymph nodes were investigated by FACS analysis for activation markers CD44 and CD69 and cytokines IL-6 and IL-4. Numbers denote percentage of cells within the ranges indicated by brackets. *$P < 0.05$, #$P < 0.01$ versus wild type.

because this symptom is critical for the differential diagnosis of OS from other causes of SCID. The levels of serum IgE in the double-mutant CD4 KO mice were similar to those in normal mice and substantially reduced compared with the single-mutant MM mice (Figure 8). Double-mutant MM mice lacking IL-4, IL-6, and CD40 likewise had much lower levels of serum IgE than did single-mutant MM mice (Figure 8). Because we showed that the homeostatic proliferating CD4+ T cells in MM mice expressed high levels of IL-4 and IL-6, and it was previously reported that CD40–CD40 ligand (CD40-CD40L) is a critical T cell–B cell signaling mechanism for Ig expression (24, 25), these results strongly suggest that T cell–B cell interactions via cytokines and adhesion molecules are

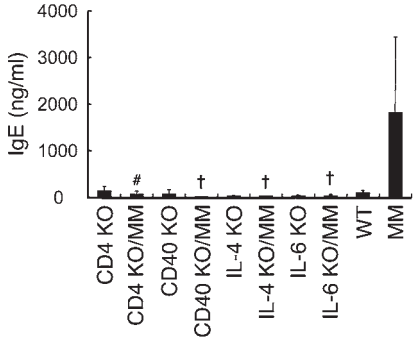

Figure 8

$CD4^+$ T cells play a role in the hyper-IgE state in MM mice. MM mice were crossed with CD4, CD40, IL-4, or IL-6 KO mice to obtain double-mutant CD4, CD40, IL-4, and IL-6 KO MM mice (KOMM), and the serum concentration of IgE in these double-mutant mice was determined. Results are mean and SD of 4 mice. The concentration of IgE in the serum was decreased in the double-mutant mice compared with MM mice (CD4KOMM, $P = 0.006$; CD40KOMM, $P < 0.001$; IL-4KOMM, $P < 0.001$; and IL-6KOMM, $P < 0.001$). $^{\#}P < 0.01$, $^{\dagger}P < 0.001$ versus wild type.

involved in the upregulation of serum IgE concentration in MM mice. Together, these results suggest that the homeostatically proliferating $CD4^+$ T cells that express excess cytokines are critical for the induction of the hyper-IgE state in MM mice and, by extension, contribute to the symptoms of OS.

Discussion

Here we describe the identification and characterization of an apparently spontaneous mutation in the gene coding for *Rag1* in a stock C57BL/10 mouse from The Jackson Laboratory. We originally identified 1 female C57BL/10 mouse carrying an abnormally high percentage of memory-phenotype $CD8^+$ T cells and named it the MM mouse. We observed that the levels of both T and B cells were lower in MM than in wild-type mice and that its primary mutation affected a step in which rearrangement is critical for the maturation of T and B cells.

The mutation in the MM mouse turned out to be a point mutation (G to A) in the *Rag1* gene and led to an amino acid change from arginine to glutamine at residue 972 in the core domain of the Rag1 molecule. The core domain of Rag1 has been defined as the minimal region required for its recombination activity (26, 27). Here we demonstrated that mouse Rag1 expressing the MM mutation had about 12% the Rag1 activity of the wild-type enzyme. The molecular mechanism of reduced Rag1 activity in MM mice might be explained by the previously published results of Roth and colleagues (28). They prepared a mutant Rag1 with an amino acid substitution at the R972 residue and demonstrated that Rag complexes carrying the mutant Rag1 molecules nicked DNA at wild-type levels but were severely impaired in their ability to catalyze DNA hairpin formation (14% of wild-type level). Therefore, it is reasonable to postulate that the mutant Rag1 molecules in MM mice have similarly reduced activity in the same function.

Interestingly, a change in human Rag1 identical to that of MM mice, of arginine to glutamine at position 975, has been reported in 1 allele of a patient with OS (15). In this patient the other allele of Rag1 was rendered relatively nonfunctional by a mutation leading to the change R396L (15). This patient had clinical features typical of OS (erythroderma, skin rash, pneumonia, lymphadenopathy, hepatomegaly, splenomegaly, and protracted diarrhea) and also expressed typical immunological phenotypes of the syndrome (decreased numbers of lymphocytes, increased numbers of eosinophils, and elevated serum IgE) (15). Some of these clinical features and immunological phenotypes are very similar to those in the MM mice. Thus, we believe that the MM mouse provides a novel animal model of human OS.

The MM mouse model allowed us to demonstrate — for the first time to our knowledge — that the skin redness, hepatomegaly, splenomegaly, decreased number of lymphocytes, increased number of eosinophils, and elevated serum IgE, all of which are characteristic of OS in humans, were dependent on the *Rag* mutation and not on other genetic factors. Additionally, we hypothesize that the other phenotypes observed in the patient described above, but not in the MM mice (e.g., pneumonia, lymphadenopathy, protracted diarrhea, and the T cell pool expansion associated with organomegaly, skin, and gut infiltration), are induced by other factors such as infection, genetic predisposition, or environmental factors.

It has well been established that in humans the same *RAG* mutations may lead to different symptoms, T^-B^- SCID or OS, and that this variability may even be observed within the same family (15, 17, 29). These observations strongly suggest that the phenotypic manifestations of OS reflect the interaction between genetic and environmental factors. However, it should be noted that although they are specific pathogen–free, there is some variation in the phenotypes of the MM mice, even amongst those housed together (Supplemental Figure 10). Therefore, either there are unsuspected variations in the environment of our mice, or stochastic factors such as the specificities for antigen of the B and/or T cells that expand oligoclonally in these mice also affect the phenotype of this disease. Further studies are required to evaluate this possibility.

Eighty percent of patients with OS, as reported by Alleman et al. (12), and a majority of patients with OS (more than 80%, including the patient described above), as reported by Villa et al. (15), had low levels of IgM or/and IgG in their sera compared with normal individuals. However, MM mice have higher than normal levels of these antibody isotypes. We do not know why these levels would differ between humans and mice with essentially the same genetic deficiency. It might be due to the fact that we are studying a particular point mutation in *Rag*, which differs from the mutations in almost all human OS patients. In this regard it is worth noting that the residual V(D)J activity of the Rag1 mutant protein in MM mice is higher, at 12% of control, than that observed in most patients with OS. Perhaps this allows the generation of enough B cells to fill up the peripheral pool and provide normal or higher levels of serum Ig. On the other hand, the difference in Ig levels between MM mice and patients with OS may be a result of their different environments (specific pathogen–free versus conventional) or of some species-specific adaptation to the RAG mutation. Further studies are needed to resolve this discrepancy.

OS and the MM mice are characterized by high levels of IgE. These high levels are probably responsible for many manifestations of the disease. The high levels of IgE could be caused either by some direct effect of RAG1 insufficiency on B cells, or indirectly, via an effect on low RAG1 activity on T cells. Of these 2 hypotheses, our present results support the latter: serum IgE did not rise above the levels observed in normal mice when the MM mice lacked IL-4, CD40, or IL-6. All of these factors, 2 of which are T cell dependent, have been shown to be critical for

the development of Ig-secreting cells (24, 25, 30, 31). In normal mice, homeostatic proliferation is manifest only during the neonatal period, when thymus-derived naive T cells first migrate into the lymphopenic peripheral environment (32). However, we and others have previously demonstrated that dysregulated homeostatic proliferation of $CD4^+$ T cells can play a role in the development of autoimmune diseases and that homeostatically proliferating $CD4^+$ T cells produce factors that are critical for their development (22, 23). Homeostatic proliferation of $CD4^+$ T cells (MM $CD4^+$ or wild-type $CD4^+$ T cells, regardless of their source) was enhanced in the MM mice compared with controls, even without induction of lymphopenic conditions, and the $CD4^+$ T cells in the MM mice expressed more Th2 cytokines than did those of wild-type mice. Taking all these data together, we suggest that the relatively lymphopenic environment of MM mice allows uncontrolled homeostatic proliferation of T cells that would be under tighter control in normal mice. In turn, the aberrantly proliferating cells differentiate to Th2 cells, perhaps via a default pathway, and produce abnormally high levels of Th2 cytokines, thus leading to downstream production of IgE and other manifestations of OS. This scenario probably also applies to human patients with OS. Thus, as has previously been suggested (33), OS is caused by mutations in *RAG* that lead to marginal activity of the enzyme, and the differences between the symptoms of OS and SCID are caused by low production of CD4 T cells in patients with the former disease, versus complete absence of CD4 T cells in patients with the latter. In support of this idea, it should be noted that OS has also been seen in humans with hypomorphic mutations in other genes, including *Artemis* (34), *RMRP* (35), and *IL-7Rα* chain (36), as well as in patients with atypical DiGeorge syndrome (37). All of these mutations cause lymphopenia and thus support our idea that OS is caused at least in part by a lymphopenia condition that is able to enhance dysregulated homeostatic proliferation of $CD4^+$ T cells.

In summary, we have discovered what we believe to be a novel mouse model of OS, the MM mouse. MM mice have a mutation in the core region of the Rag1 protein. Using this OS model, we demonstrated that erythroderma, hepatosplenomegaly, hypereosinophilia, elevated serum IgE levels, excess activated $CD4^+$ T cells, and oligoclonal Vβ usage of T cells were a direct consequence of the *Rag* mutation. Moreover, we showed that the $CD4^+$ T cells of the MM mice were homeostatically proliferating, expressed high levels of Th2 cytokines, and were involved in the development of the hyper-IgE state, a critical symptom in the differential diagnosis of OS versus SCID patients. Thus, we conclude that dysregulated homeostatic proliferating $CD4^+$ T cells are involved in the pathogenesis of OS.

Methods

Mice. C57BL/6, C57BL/10, BALB/c, and NZB mice were purchased from The Jackson Laboratory and Japan SLC. We obtained CD4 KO (38) and IL-4 KO (39) mice from The Jackson Laboratory, IL-6 KO (40) mice from Y. Iwakura (University of Tokyo, Tokyo, Japan), and CD40 KO (41) mice from H. Kikutani (Osaka University). Mice were maintained in the animal facilities of the National Jewish Medical and Research Center and Osaka University under specific pathogen–free conditions. Animal experiments were approved by the Institutional Animal Care and Use Committees of the National Jewish Medical and Research Center and by the Graduate School of Frontier Biosciences and the Graduate School of Medicine of Osaka University. Most of the mice used were 5–8 weeks old.

Antibodies and reagents. The following allophycocyanin-conjugated (APC-conjugated) mAbs were used: anti-CD4 (BioLegend); anti-CD8 and anti-CD19 (BD); and anti-TCRβ and anti-IgM (eBioscience). The following FITC-conjugated mAbs were used: anti-CD4, anti-CD8, and anti-CD11c (BioLegend); anti–Gr-1, anti-CD11b, anti-B220, and anti-IgM (eBioscience); anti-NK1.1 and anti–GL-7 (BD); and anti-CD69 (CALTAG). The following PE-conjugated mAbs were used: anti-CD4, anti-CD8, anti-CD44, anti-CD122, anti-CD11c, anti-CD11b, and anti-IgD (eBioscience); anti-CD25 (CALTAG); anti-CCR3 (R&D Systems); and anti-CD43, anti-B220, anti-NK1.1, anti–TCR-β, anti–TCR-γδ, anti–IL-4, anti–IL-6, anti–IL-10, anti–IL-2Rα, anti-IgG1, and anti-IgM (BD). The following Cy5-conjugated mAbs were used: anti-CD44 and anti-B220 (BD); anti-CD11c, anti-CD8, anti–IL-2Rβ, and anti-CD19 (eBioscience); and anti-CD11b and anti-CD69 (BioLegend). The remaining mAbs used were as follows: Tri-color–conjugated anti-B220 (CALTAG); biotin-conjugated anti-PNA (Honen Corporation–Japan); and streptavidin-APC (BioLegend).

Fluorescence-activated cell sorter analysis. Thymocytes, splenocytes, and bone marrow cells were prepared and incubated with fluorescent-conjugated antibodies (for specific staining and dump staining). Fluorescence-activated cell sorter (FACS) analysis was performed on a FACSCalibur (BD) or a CyAn flow cytometer (DakoCytomation).

Hematological analysis. The PBLs of each mouse were collected and analyzed for the total number of red blood cells, white blood cells, platelets, and lymphocytes by the Research Institute for Microbial Diseases of Osaka University.

Bone marrow transplantation. Bone marrow transplantation was performed as described previously (23) using MM and wild-type mice.

Chromosome mapping. MM mice were crossed with NZB mice and intercrossed to produce F2 offspring. Genomic DNA was isolated from their livers. For the first screening, DNA pooled from 10–12 phenotype-positive or -negative F2 offspring was prepared. The inherited C57BL/10 regions were mapped with microsatellite markers that have been previously described to be polymorphic between C57BL/10 and NZB (42–45). After chromosome 2 was identified as containing the mutation, we performed the second screening using nonpooled DNA.

Expression vectors. Wild-type Rag1 (M6) or Rag2 (MR2) cDNA (46) (generous gifts from D.G. Schatz, Yale University, New Haven, Connecticut, USA) was subcloned into a modified pEF-BOS vector (47). Mutant Rag1 was amplified by PCR from the mutant mice and introduced into a pEF-BOS-EX expression vector (pBOS-Rag1). The fidelity of the PCR and subcloning was confirmed by DNA sequencing.

In vitro recombination assay. To measure the catalytic activity of the mutant protein, transient expression of the recombination activity was determined by a modified assay that was described previously (6, 46).

ELISA. Serum antibody titers were determined by ELISA for IgE (BD); IgA, IgM, and IgG (Zymed Laboratories); and IgG (Southern Biotechnology).

Cell preparation and sorting. The lymph nodes and spleens from MM and wild-type mice were harvested, and $CD4^+CD44^{low}$ and $CD8^+CD44^{low}$ T cells were purified using a MoFlo cell sorter (DakoCytomation). The purity of the $CD4^+$ and $CD8^+$ T cells was consistently greater than 98%.

Homeostatic proliferation assay. $CD44^{low}$ T cells were labeled with CFSE (Invitrogen) and injected i.p. (5×10^5 cells) into 3-day-old neonatal or i.v. (3×10^6 cells) into 8-week-old adult wild-type and MM mice. The recipients were sacrificed for analysis 21 days after injection.

Cytokine intracellular staining. The T cell–enriched fractions from lymph nodes and spleens were stimulated with anti-CD3 and anti-CD28 in the presence of Golgi-Stop (BD Biosciences) for 5 hours, stained with anti-CD4 or anti–TCR-β, and fixed and permeabilized using BD Cytofix/Cytoperm (BD Biosciences), followed by anti–IL-4, anti–IL-6, or anti–IL-10 staining.

Western blotting. Nuclear fractions of the sorted cell populations were prepared by a kit (Sigma-Aldrich). The nuclear fractions were resolved by 10%–20% SDS-PAGE, and the protein fraction was applied on Western blotting analysis with anti-mouse Rag1 antibody (Santa Cruz Biotechnology Inc.) plus HRP-conjugated secondary antibody (Zymed Laboratories) and visualized by ECL (Amersham).

In vitro proliferation assay. For in vitro proliferation assay of T cells, $CD4^+$ and $CD8^+$ T cells of MM and wild-type mice were sorted and cultured in the presence or absence of anti-CD3 and anti-CD28 mAbs (BD). Anti-CD3 and anti-CD28 mAbs (both at 0.625, 1.25, 2.5, 5, or 10 μg/ml) were coated at 37°C for 3 hours, and the resulting plates were washed with PBS twice. The resulting cells were plated in anti-CD3–coated 96-well plates at a concentration of 1×10^5 cells/well in RPMI-1640 medium supplemented with 10% FCS. For B cells, $B220^+CD19^+$ B cells of MM and wild-type mice were sorted and cultured in the presence or absence of LPS (Sigma-Aldrich). Two days later, 20 μl of 5 mg/ml 3-(4,5-dimethyl-2-thiazolyl)-2,5-diphenyl-2H-tetrazolium bromide (MTT) in PBS were added to each well. After 4 hours at 37°C, cell proliferation was measured by MTT assay.

Pathological examination. Thymi, spleens, livers, skin, and intestines of both wild-type and MM mice were fixed with 10% paraformaldehyde in normal saline buffer overnight. After the paraformaldehyde was replaced with PBS, the fixed organs were dehydrated with a serial dilution of alcohol, embedded in paraffin wax, subjected to section, and stained with H&E. Slides were examined pathologically under a microscope.

In vivo immunization of TD and TI antigens. To examine the TI responses, 8-week-old MM and wild-type mice were injected i.p. with 50 μg TNP-LPS (prepared in this laboratory). For the TD responses, the mice were i.p. injected with 100 μg DNP-KLH (LSL) precipitated with 4 mg alum (LSL), assigned as day 0, and were boosted with 20 μg of DNP-KLH in saline on day 21. Blood was taken through the retroorbital plexus every 7 days, and antibody production was determined by ELISA.

Analysis of germinal center B cells. TD antigen–immunized or control MM and wild-type mice were sacrificed on day 28 after the treatment, and splenocytes were prepared and subjected to FACS analysis for germinal center B cells.

Oligonucleotides. For IgM spectratyping, oligonucleotides specific for murine *V_hJ558* and *V_hQ52* (as variable region) and the 2 5′-FAM–labeled J_h runoff primers has been described previously (48, 49). For immunoscope analysis of TCR, oligonucleotides specific for murine *V*α and *V*β and the 2 5′-FAM–labeled–C gene (*V*α and *V*β) runoff primers has been previously described (50).

Spectratyping. Total RNA from spleens of wild-type and MM mice were extracted using RNeasy Mini Kit (QIAGEN) and subjected for cDNA synthesis using M-MLV reverse transcriptase kit (Sigma-Aldrich). For IgM spectratyping, PCR and runoff reactions were performed as previously described (48, 49). For TCR spectratyping, PCR and runoff reactions were performed as previously described (50). Briefly, PCR reactions with specific *V_h* and *IgM* primers or *V*α or *V*β with *C* gene primers were performed, and the PCR products were visualized on a 1.5% agarose gel with ethidium bromide before using 2 or 5 μl of the PCR products for runoff elongations with the fluorescent *J_h* primers for IgM or the fluorescent C gene primer for *TCR*, respectively. The elongation products (2 μl), together with 0.5 μl of GeneScan lane standard (400HD ROX; Applied Biosystems), were loaded onto automated DNA sequencer (model 301; Applied Biosystems). Size determination and *CDR3* size analysis were performed using the GeneScan software package (version 3.1; Applied Biosystems).

Statistics. Student's *t* test (2-tailed) was used for the statistical testing between 2 groups. A *P* value less than 0.05 was considered significant.

Acknowledgments

We are grateful to E. Iketani and T. Hayashi (Osaka University) for their excellent technical assistance, and we thank R. Masuda (Osaka University) for her excellent secretarial assistance. We are grateful to Y. Inoue and T. Tanaka (Osaka University) for their excellent technical assistance in sequencing. This work was supported by Grants-in-Aid for Scientific Research from the Ministry of Education, Culture, Sports, Science, and Technology of Japan (to M. Murakami and T. Hirano) and from the Osaka Foundation for the Promotion of Clinical Immunology (to M. Murakami and T. Hirano) as well as by US Public Health Service grants AI-17134, AI-19785, and AI-52225 to P. Marrack and J. Kappler.

Received for publication September 29, 2006, and accepted in revised form February 20, 2007.

Address correspondence to: Masaaki Murakami, Department of Developmental Immunology, Graduate School of Medicine, Osaka University, 2-2, Yamada-oka, Suita, Osaka 565-0871, Japan. Phone: 81-6-6879-3881; Fax: 81-6-6879-3889; E-mail: murakami@molonc.med.osaka-u.ac.jp.

Khie Khiong and Masaaki Murakami contributed equally to this work.

Philippa Marrack and Toshio Hirano contributed equally to this work.

1. Fugman, S.D., Villey, I.J., Ptaszek, L.M., and Schatz, D.G. 2000. Identification of two catalytic residues in Rag1 that define a single active site within the Rag1/Rag2 protein complex. *Mol. Cell.* **5**:97–107.
2. Landree, M.A., Wibbenmeyer, J.A., and Roth, D.B. 1999. Mutational analysis of Rag1 and Rag2 identifies three catalytic amino acids in Rag1 critical for both cleavage steps of V(D)J recombination. *Genes Dev.* **13**:3059–3069.
3. Roth, D.B., Zhu, C., and Gellert, M. 1993. Characterization of broken DNA molecules associated with V(D)J recombination. *Proc. Natl. Acad. Sci. U. S. A.* **90**:10788–10792.
4. Steen, S.B., Gomelsky, L., and Roth, D.B. 1996. The 12/23 rule is enforced at the cleavage step of V(D)J recombination in vivo. *Genes Cells.* **1**:543–553.
5. Steen, S.B., Gomelsky, L., Speidel, S.L., and Roth, D.B. 1997. Initiation of V(D)J recombination in vivo: role of recombination signal sequences in formation of single and paired double-strand breaks. *EMBO J.* **16**:2656–2664.
6. Oettinger, M.A., Schatz, D.G., Gorka, C., and Baltimore, D. 1990. Rag1 and Rag2, adjacent genes that synergistically activate V(D)J recombination. *Science.* **248**:1517–1523.
7. Mombaerts, P., et al. 1992. RAG-1-deficient mice have no mature B and T lymphocytes. *Cell.* **68**:869–877.
8. Shinkai, Y., et al. 1992. RAG-2-deficient mice lack mature lymphocytes owing to inability to initiate V(D)J rearrangement. *Cell.* **68**:855–867.
9. Schwarz, K., et al. 1996. Rag mutations in human B cell-negative SCID. *Science.* **274**:97–99.
10. Santagata, S., Villa, A., Sobacchi, C., Cortes, P., and Vezzoni, P. 2000. The genetic and biochemical basis of Omenn syndrome. *Immunol. Rev.* **178**:64–74.
11. Omenn, G.S. 1965. Familial reticuloendotheliosis with eosinophilia. *N. Engl. J. Med.* **273**:427–432.
12. Aleman, K., Noordzij, J.G., de Groot, R., van Dongen, J.J., and Hartwig, N.G. 2001. Reviewing Omenn syndrome. *Eur. J. Pediatr.* **160**:718–725.
13. Villa, A., Sobacchi, C., and Vezzoni, P. 2002. Omenn syndrome in the context of other B cell-negative severe combined immunodeficiencies. *Isr. Med. Assoc. J.* **4**:218–221.
14. Villa, A., et al. 1998. Partial V(D)J recombination activity leads to Omenn syndrome. *Cell.* **93**:885–896.
15. Villa, A., et al. 2001. V(D)J recombination defects in lymphocytes due to RAG mutations: severe immunodeficiency with a spectrum of clinical presentations. *Blood.* **97**:81–88.
16. Sobacchi, C., Marrella, V., Rucci, F., Vezzoni, P., and Villa, A. 2006. RAG-dependent primary immunodeficiencies. *Hum. Mutat.* **27**:1174–1184.
17. de Saint-Basile, G., et al. 1991. Restricted heterogeneity of T lymphocytes in combined immunodeficiency with hypereosinophilia (Omenn's syndrome). *J. Clin. Invest.* **87**:1352–1359.
18. Businco, L., et al. 1987. Clinical and immunological findings in four infants with Omenn's syndrome: a form of severe combined immunodeficiency with phenotypically normal T cells, elevated IgE, eosinophilia. *Clin. Immunol. Immunopathol.* **44**:123–133.
19. Bruckmann, C., et al. 1991. Severe pulmonary vascular occlusive disease following bone marrow transplantation in Omenn syndrome. *Eur. J. Pediatr.*

150:242–245.
20. Melamed, I., Cohen, A., and Roifman, C.M. 1994. Expansion of CD3+CD4-CD8- T cell population expressing high levels of IL-5 in Omenn's syndrome. *Clin. Exp. Immunol.* **95**:14–21.
21. Goldrath, A.W., Bogatzki, L.Y., and Bevan, M.J. 2000. Naive T cells transiently acquire a memory-like phenotype during homeostasis-driven proliferation. *J. Exp. Med.* **192**:557–564.
22. King, C., Ilic, A., Koelsch, K., and Sarvetnick, N. 2004. Homeostatic expansion of T cells during immune insufficiency generates autoimmunity. *Cell.* **117**:265–277.
23. Sawa, S., et al. 2006. Autoimmune arthritis associated with mutated interleukin (IL)-6 receptor gp130 is driven by STAT3/IL-7-dependent homeostatic proliferation of $CD4^+$ T cells. *J. Exp. Med* **203**:1459–1470.
24. Foy, T.M., et al. 1996. Immune regulation by CD40 and its ligand gp39. *Annu. Rev. Immunol.* **14**:591–617.
25. Banchereau, F.B., et al. 1994. The CD40 antigen and its ligand. *Annu. Rev. Immunol.* **12**:881–922.
26. Cortes, P., Ye, Z., and Baltimore, D. 1994. Rag1 interacts with the repeated amino acids motif of the human homologue of the yeast protein SRP1. *Proc. Natl. Acad. Sci. U. S. A.* **91**:7633–7637.
27. McMahan, C.J., Difilippantonio, M.J., Rao, N., Spanopoulou, E., and Schatz, D.G. 1997. A basic motif in the N-terminal region of RAG1 enhances V(D)J recombination activity. *Mol. Cell. Biol.* **17**:4544–4552.
28. Lu, C.P., Sandoval, H., Brandt, V.L., Rice, P.A., and Roth, D.B. 2006. Amino acid residues in Rag1 crucial for DNA hairpin formation. *Nat. Struct. Mol. Biol.* **13**:1010–1015.
29. Corneo, B., et al. 2001. Identical mutations in RAG1 or RAG2 genes leading to defective V(D)J recombinase activity can cause either T-B-severe combined immune deficiency or Omenn syndrome. *Blood.* **97**:2772–2776.
30. Finkelman, F.D., et al. 1990. Lymphokine control of in vivo immunoglobulin isotype selection. *Annu. Rev. Immunol.* **8**:303–333.
31. Hirano, T. 1998. Interleukin 6 and its receptor: ten years later. *Int. Rev. Immunol.* **16**:249–284.
32. Min, B., et al. 2003. Neonates support lymphopenia-induced proliferation. *Immunity.* **18**:131–140.
33. Schandene, L., et al. 1993. T helper type 2-like cells and therapeutic effects of interferon-gamma in combined immunodeficiency with hypereosinophilia (Omenn's syndrome). *Eur. J. Immunol.* **23**:56–60.
34. Ege, M., et al. 2005. Omenn syndrome due to ARTEMIS mutations. *Blood.* **105**:4179–4186.
35. Roifman, C.M., Gu, Y., and Cohen, A. 2006. Mutations in the RNA component of RNase mitochondrial RNA processing might cause Omenn syndrome. *J. Allergy Clin. Immunol.* **117**:897–903.
36. Giliani, S., et al. 2006. Omenn syndrome in an infant with IL7RA gene mutation. *J. Pediatr.* **148**:272–274.
37. Markert, M.L., et al. 2004. Complete DiGeorge syndrome: development of rash, lymphadenopathy, and oligoclonal T cells in 5 cases. *J. Allergy Clin. Immunol.* **113**:734–741.
38. Rahemtulla, A., et al. 1991. Normal development and function of CD8+ cells but markedly decreased helper activity in mice lacking CD4. *Nature.* **353**:180–184.
39. Kopf, M., et al. 1993. Disruption of the murine IL-4 gene blocks TH2 cytokine responses. *Nature.* **362**:245–248.
40. Park, S.J., et al. 2004. IL-6 regulates in vivo dendritic cell differentiation through STAT3 activation. *J. Immunol.* **173**:3844–3854.
41. Kawabe, T., et al. 1994. The immune responses in CD40-deficient mice: impaired immunoglobulin class switching and germinal center formation. *Immunity.* **1**:167–178.
42. Rozzo, S.J., Vyse, T.J., Drake, C.G., and Kotzin, B.L. 1996. Effect of genetic background on the contribution of New Zealand black loci to autoimmune lupus nephritis. *Proc. Natl. Acad. Sci. U. S. A.* **93**:15164–15168.
43. Rozzo, S.J., Vyse, T.J., Menze, K., Izui, S., and Kotzin, B.L. 2000. Enhanced susceptibility to lupus contributed from the nonautoimmune C57BL/10, but not C57BL/6, genome. *J. Immunol.* **164**:5515–5521.
44. Vyse, T.J., et al. 1998. Contributions of Ea(z) and Eb(z) MHC genes to lupus susceptibility in New Zealand mice. *J. Immunol.* **160**:2757–2766.
45. Vyse, T.J., Halterman, R.K., Rozzo, S.J., Izui, S., and Kotzin, B.L. 1999. Control of separate pathogenic autoantibody responses marks MHC gene contributions to murine lupus. *Proc. Natl. Acad. Sci. U. S. A.* **96**:8098–8103.
46. Hesse, J.E., Lieber, M.R., Gellert, M., and Mizuuchi, K. 1987. Extrachromosomal DNA substrates in pre-B cells undego inversion or deletion at immunoglobulin V(D)J joining signals. *Cell.* **49**:775–783.
47. Mizushima, S., and Nagata, S. 1990. pEF-BOS, a powerful mammalian expression vector. *Nucleic Acids Res.* **18**:5322.
48. Delassus, S., et al. 1995. PCR-based analysis of the murine immunoglobulin heavy-chain repertoire. *J. Immunol. Methods.* **184**:219–229.
49. LeMaoult, J., et al. 1997. Clonal expansions of B lymphocytes in old mice. *J. Immunol.* **159**:3866–3874.
50. Currier, J.R., and Robinson, M.A. 2000. Spectratype/immunoscope analysis of the expressed TCR repertoire. In *Current protocols in immunology*. J.E. Coligan, A.M. Kruisbeek, D.H. Margulies, E.M. Shevach, and W. Strober, editors. John Wiley. New York, New York, USA. 10.28.1–10.28.24.